2015

Pauli-limited effect in the magnetic phase diagram of FeSexTe1−x thin films

Jincheng Zhuang
University of Wollongong, jz673@uowmail.edu.au

Zhen Li
University of Wollongong, zhenl@uow.edu.au

Xun Xu
University of Wollongong, xun@uow.edu.au

Li Wang
University of Wollongong, lw037@uowmail.edu.au

Wai Kong Yeoh
University of Wollongong, wyeoh@uow.edu.au

See next page for additional authors

Pauli-limited effect in the magnetic phase diagram of FeSexTe1−x thin films

Abstract

We present a detailed investigation on the doping dependence of the upper critical field $H_{c2}(T)$ of FeSexTe1−x thin films $(0.18 \leq x \leq 0.90)$ by measuring the electrical resistivity as a function of magnetic field. The $H_{c2}(T)$ curves exhibit a downturn behavior with decreasing temperature in all the samples, owing to the Pauli-limited effect (spin paramagnetic effect). The Pauli-limited effect on the upper critical field can be monotonically modulated by variation of the Se/Te composition. Our results show that Te-doping induced disorder and excess Fe atoms give rise to enhancement of the Pauli-limited effect.

Authors

Jincheng Zhuang, Zhen Li, Xun Xu, Li Wang, Wai Kong Yeoh, X Z. Xing, Zhixiang Shi, Xiaolin Wang, Yi Du, and S X. Dou

Pauli-limited effect in the magnetic phase diagram of FeSexTe1−x thin films

J. C. Zhuang, Z. Li, X. Xu, L. Wang, W. K. Yeoh, X. Z. Xing, Z. X. Shi, X. L. Wang, Y. Du, and S. X. Dou

Articles you may be interested in

Unusual microwave response and bulk conductivity of very thin FeSe0.3Te0.7 films as a function of temperature
Low Temp. Phys. **40**, 492 (2014); 10.1063/1.4881178

Properties of high-angle Fe(Se,Te) bicrystal grain boundary junctions
Appl. Phys. Lett. **104**, 162601 (2014); 10.1063/1.4871864

Pressure effects on the superconducting thin film Ba1− x K x Fe2As2
Appl. Phys. Lett. **101**, 042601 (2012); 10.1063/1.4738783

Pressure effects on strained FeSe0.5Te0.5 thin films
J. Appl. Phys. **111**, 112610 (2012); 10.1063/1.4726209

Pressure effects on superconductivity of Fe 1 + y Te 1 − x S x single crystals
J. Appl. Phys. **107**, 083903 (2010); 10.1063/1.3385392

Pauli-limited effect in the magnetic phase diagram of FeSe$_x$Te$_{1-x}$ thin films

J. C. Zhuang,[1] Z. Li,[1] X. Xu,[1] L. Wang,[1] W. K. Yeoh,[1] X. Z. Xing,[2] Z. X. Shi,[2,a)] X. L. Wang,[1] Y. Du,[1,a)] and S. X. Dou[1,a)]

[1]*Institute for Superconducting and Electronic Materials, University of Wollongong, North Wollongong, New South Wales 2500, Australia*
[2]*Department of Physics and Key Laboratory of MEMS of the Ministry of Education, Southeast University, Nanjing 211189, People's Republic of China*

We present a detailed investigation on the doping dependence of the upper critical field $H_{c2}(T)$ of FeSe$_x$Te$_{1-x}$ thin films ($0.18 \leq x \leq 0.90$) by measuring the electrical resistivity as a function of magnetic field. The $H_{c2}(T)$ curves exhibit a downturn behavior with decreasing temperature in all the samples, owing to the Pauli-limited effect (spin paramagnetic effect). The Pauli-limited effect on the upper critical field can be monotonically modulated by variation of the Se/Te composition. Our results show that Te-doping induced disorder and excess Fe atoms give rise to enhancement of the Pauli-limited effect. © 2015 AIP Publishing LLC. [http://dx.doi.org/10.1063/1.4936848]

The discovery of iron-based superconductors (IBSs) has generated great interest in the condensed-matter physics community due to the high superconducting transition temperature (T_C) and unconventional pairing mechanism.[1–3] As one fundamental superconducting parameter, the upper critical field, H_{c2}, is very important for understanding the superconducting properties. The temperature dependence of H_{c2}, $H_{c2}(T)$, reflects the details of the underlying electronic structures and provides insights into the microscopic origin of the pairing strength and pair-breaking mechanism, which is critical for potential application of the IBSs. Nevertheless, no single common characteristic could be generalized to explain the $H_{c2}(T)$ behavior in the IBSs, even in the same group. The curvature of $H_{c2}(T)$ displays a clear upward trend for the 1111 system, ReFeAsF$_x$O$_{1-x}$ (Re = rare earth), which is attributed to the presence of multiband effects.[4,5] Nevertheless, a sharp increase in $H_{c2}(T)$ near T_C, combined with saturation at low temperature, was observed in oxygen deficient LaFeAsO samples, which are mainly affected by the spin-paramagnetic effect.[6,7] Furthermore, the spin-paramagnetic effect was also revealed in LiFeAs.[8] For the electron- or hole-doped 122 system, AFe$_2$As$_2$ (A = Ba, Sr, and Ca), $H_{c2}(T)$ exhibits a linear increase down to temperature far away from T_C,[9–11] possibly evoked by the band-warping effect. The complexity of the structure and the introduced charge carriers act as a barrier to the investigation of intrinsic $H_{c2}(T)$ properties in these systems.

Another type of IBSs, the iron chalcogenides FeCh (Ch = Se, Te) in the 11 system, has been discovered with $T_C \sim 8$ K.[12,13] In view of the simple crystal structure, composed of a one-stack superconducting layer along the c-axis,[12] and similarity in the band structure compared with the other IBSs,[14,15] FeCh is taken as a model system to study the superconducting mechanism. The behavior of $H_{c2}(T)$ of FeSe could be described well by the Werthamer-Helfand-Hohenberg (WHH) theoretical curve in the orbit limited situation.[16] For high Te content FeSe$_x$Te$_{1-x}$ samples ($x < 0.5$), the Pauli paramagnetic effect dominates the $H_{c2}(T)$

shape.[17,18] Nevertheless, the origin of the pair-breaking mechanism in the 11 system remains mysterious, due to the fact that there has been no investigation on the $H_{c2}(T)$ behavior of samples in the range of $0.6 < x < 0.9$, which bridge the region between the pure FeSe sample and the high Te content samples ($x \leq 0.5$). This is caused by the difficulty in producing high quality samples in this special region, where polycrystalline samples are found to have multiple phases,[13] while pure single crystal samples have never been fabricated. Thus, high quality samples are urgently needed to reveal the pair-breaking mechanism in this system.

In this paper, we present a systematic characterization of $H_{c2}(T)$ in FeSe$_x$Te$_{1-x}$ thin films ($0.18 \leq x \leq 0.90$), overcoming the phase separation issue in bulk and single crystal samples via the pulsed laser deposition (PLD) method. A strong bending effect on $H_{c2}(T)$ was observed in high Te composition samples. The $H_{c2}(T)$ curves can be successfully described by the WHH prediction, considering the spin-parameter effect. Microstructure characterization implies that the Te dopant introduces disorder, which modulates the Pauli-limited effect in this system.

Polycrystalline pellets of FeTe$_{1-x}$Se$_x$ with nominal compositions in the range of $0.18 \leq x \leq 0.90$ were fabricated as targets. Powders of Fe, Se, and Te were mixed together in stoichiometric ratios and heated in an evacuated quartz tube at 850 °C for 12 h. After the sintering, the mixture was reground, pelletized, and sintered in the evacuated quartz tube at 400 °C for 6 h to make the target dense. The films were grown under high vacuum conditions ($\sim 4 \times 10^{-4}$ Pa) by PLD using a Nd:yttrium aluminum garnet (Nd:YAG) laser, as reported elsewhere.[19,20] Single crystal CaF$_2$ (100) with lattice parameter $a_0 = 5.463$ Å was selected as the substrate due to its non-oxide nature and the low mismatch between its lattice parameter ($a_0/\sqrt{2} = 3.863$ Å) and the a-axis parameter of the film (around 3.8 Å). The deposition temperature was set at 450 °C, and the laser energy was 200 mJ/pulse. The substrate-target distance was maintained at 4 cm, and the deposition time was the same for all samples. The actual composition x of each film is determined by energy dispersive X-ray (EDX) measurements. The thickness

a)Authors to whom correspondence should be addressed. Electronic addresses: ydu@uow.edu.au; zxshi@seu.edu.cn; and shi@uow.edu.au.
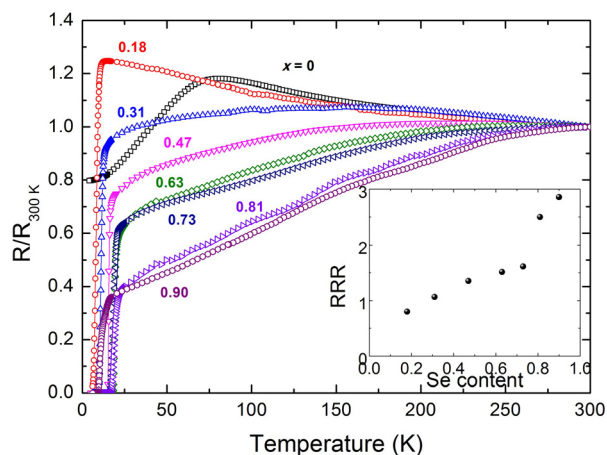
FIG. 1. Normalized electronic resistivity versus temperature (*R-T*) curves from 300 K to 2 K for all the films. Inset: Ratio of room-temperature resistivity to the residual resistivity ratio (*RRR*) as a function of Se composition.

of the films, measured by scanning electron microscopy (SEM), was around 50 nm. Only the (00*l*) reflections of thin films and substrate could be detected in the X-ray diffraction (XRD) results, indicating high purity as well as high out-of-plane orientation for all these films.[20] Electrical resistivity under different magnetic fields was measured on a 14 T physical properties measurement system (PPMS, Quantum Design). The measurements of atomic arrangement were

performed on a scanning tunneling microscopy (STM) system (USM1500-M, Unisoku Co) in ultrahigh vacuum (UHV) at 4.2 K.

Figure 1 shows the electronic resistivity versus temperature (*R-T*) curves for all the film samples, normalized by their respective resistivity at 300 K. For the un-doped FeTe film, a kink around 70 K is observed, corresponding to the antiferromagnetic (AFM) transition accompanied by a structural transition.[13] The kink disappears when the Se content increases up to $x = 0.2$, which is similar to what is found in polycrystalline samples and single crystals.[13,21] With further Se doping, the *R-T* curve in the normal state becomes more metallic, resulting in a large ratio of the room-temperature resistivity to the residual resistivity (*RRR*), as shown in the inset of Fig. 1, which stands for a clean compound.[8]

Figure 2 displays *R-T* curves under different magnetic fields, ranging from 0 T to 13 T, parallel to the *c* direction. With increasing magnetic field, the onset of the superconducting transition gradually shifts to low temperature. Broadening of the resistivity transition in magnetic field, which is the direct evidence of thermal fluctuations in a vortex system,[22] could be observed in all the films. The broadening of the widths of the superconducting transition is different, however, among different Se composition samples, where the high T_C samples ($x = 0.63$, 0.72, and 0.81) show intense field-induced broadening compared with the other

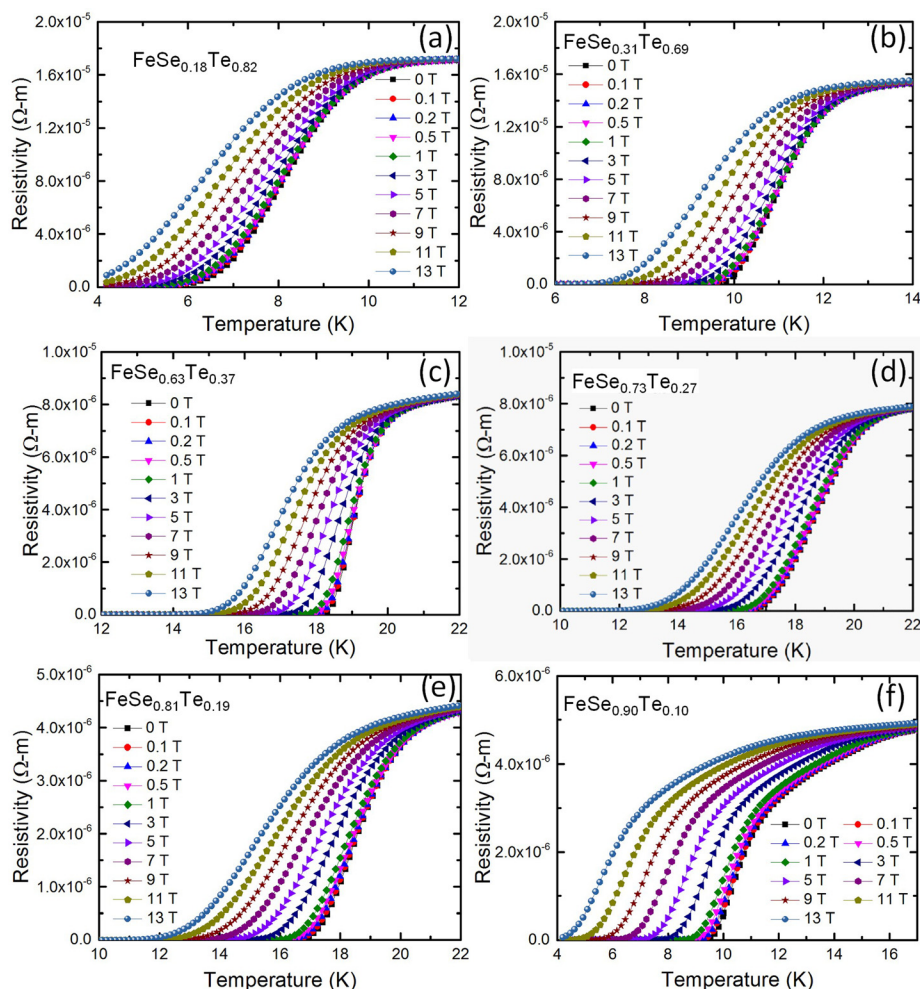FIG. 2. *R-T* curves under different magnetic fields for (a) $FeSe_{0.18}Te_{0.82}$ film, (b) $FeSe_{0.31}Te_{0.69}$ film, (c) $FeSe_{0.63}Te_{0.37}$ film, (d) $FeSe_{0.73}Te_{0.27}$ film, (e) $FeSe_{0.81}Te_{0.19}$ film, and (f) $FeSe_{0.90}Te_{0.10}$ film, respectively.

samples, suggesting the presence of a vortex-liquid region.[20] Therefore, to minimize the effects of vortex motion in the determination of H_{c2}, we used a criterion that 50% of normal state resistivity is realized at H_{c2}.

Figure 3 shows the temperature dependence of H_{c2}, with the temperature normalized to T_C. The convex shape of $H_{c2}(t)$ ($t = T/T_C$) with high slope near T_C can be seen clearly in the samples with low Se content ($x = 0.18$ and 0.31), and the bending behavior is weakened with increasing Se content. For $x = 0.90$, a linear-like behavior of $H_{c2}(t)$ with small slope is identified. The shape of the $H_{c2}(t)$ dependence on the Se composition shows that H_{c2} does not simply scale with T_C. The observed H_{c2} features indicate that the pair-breaking mechanism varies in samples with different Se/Te compositions. Generally, the Cooper pairs can be broken and destroyed by two mechanisms in a magnetic field. The first one is orbital-pair breaking, with opposite momenta acting on the paired electrons. In this case, the superconductivity is destroyed when the kinetic energy of the Cooper pairs exceeds the condensation energy. The other one is attributed to the Zeeman effect, which aligns the spins of the two electrons in the applied field (Pauli paramagnetic limit). The superconductivity is also eliminated when the Pauli spin susceptibility energy is larger than the condensation energy.

WHH theory, which could identify the contribution of each pair-breaking mechanism, was used to fit the $H_{c2}(t)$ curves, and the strength of the spin-paramagnetic effect and the spin-orbit effect was incorporated via the Maki parameter α and the spin-orbit interaction λ_{so},[23] respectively. According to the WHH theory, $H_{c2}(t)$ can be described by the digamma function[24]

$$\ln\frac{1}{t} = \left(\frac{1}{2} + \frac{i\lambda_{so}}{4\gamma}\right)\psi\left(\frac{1}{2} + \frac{\bar{h} + \lambda_{so}/2 + i\gamma}{2t}\right) + \left(\frac{1}{2} - \frac{i\lambda_{so}}{4\gamma}\right)\psi\left(\frac{1}{2} + \frac{\bar{h} + \lambda_{so}/2 - i\gamma}{2t}\right) - \psi\left(\frac{1}{2}\right), \quad (1)$$

where $\gamma \equiv [(\alpha\bar{h})^2 - (\lambda_{so}/2)^2]^{1/2}$ and $\bar{h} = \frac{4\bar{h}}{\pi^2(-dh/dt)_{t=1}}$ $= \frac{4H_{c2}}{\pi^2(-dH_{c2}/dt)_{t=1}}$.
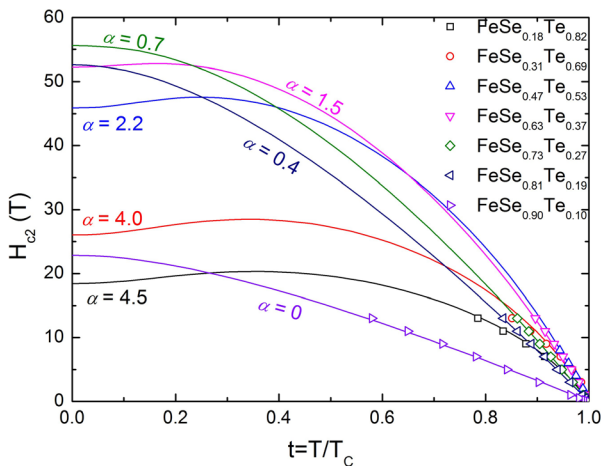

FIG. 3. Temperature dependence of the upper critical field of all superconducting films, determined using the criterion of 50% of the normal-state resistivity. The solid lines are fits to the WHH model with consideration of the spin-paramagnetic effect.

In the condition of the absence of both spin-paramagnetic effect and spin-orbit interaction, $\alpha = 0$ and $\lambda_{so} = 0$, Eq. (1) can be further treated as

$$\ln\frac{1}{t} = \psi\left(\frac{1}{2} + \frac{\bar{h}}{2t}\right) - \psi\left(\frac{1}{2}\right), \quad (2)$$

and the orbit-limited upper critical field as

$$H_{c2}^{orb}(0) = -0.69\left(\frac{dH_{c2}}{dt}\right)_{t=1}. \quad (3)$$

The WHH model described by Eq. (1) has been adopted to fit all the data, and to evaluate the value of upper critical field $H_{c2}^{WHH}(0)$ and the strength of the spin-paramagnetic effect α, assuming that $\lambda_{so} = 0$, since the spin-orbit scattering is expected to be rather weak in the FeSe$_x$Te$_{1-x}$ system.[16,17] By comparing the values of the calculated $H_{c2}^{orb}(0)$ ($\alpha = 0$) and $H_{c2}^{WHH}(0)$ ($\alpha \neq 0$), which are summarized in Table I and displayed in Fig. 4(a), we can identify the role of the spin-paramagnetic effect in the 11 system. For conventional superconductors, the upper critical field is mainly restricted by the orbital pair-breaking mechanism, where $H_{c2}^{WHH}(0)$ is comparable to $H_{c2}^{orb}(0)$. In our results, however, the calculated $H_{c2}^{WHH}(0)$ values for all films are smaller than $H_{c2}^{orb}(0)$, which is consistent with the downward trend of H_{c2} and indicates that the spin-paramagnetic effect is the predominant pair-breaking mechanism in the 11 system. It should be noted that $H_{c2}^{orb}(0)$ is much larger than $H_{c2}^{WHH}(0)$ in samples with low Se content, while $H_{c2}^{WHH}(0)$ becomes comparable to $H_{c2}^{orb}(0)$ in samples with high Se content ($x = 0.81$, 0.90), as shown in Fig. 4(a), demonstrating the enhanced spin-paramagnetic effect in films with low Se content. The calculated fitting results for α as a function of Se content are displayed in Fig. 4(b). The value of α decreases with increasing Se content, and it reaches a value of zero when $x = 0.90$, consistent with the trend in Fig. 4(a) and indicating that the spin-paramagnetic effect indeed plays a critical role in the H_{c2} curves in the 11 system.

We now focus on the origin of the variation of the spin-paramagnetic effect with changing Se/Te composition. As the unique feature in the 11 system compared to other IBSs, excess Fe in high Te component samples, which is located at the interstitial Fe(2) sites,[25,26] exhibits a larger local magnetic moment than that of normal Fe in Fe-(Se,Te) layers and leads to charge carrier localization, which is represented by the upturn trend in the $R(T)$ curves before entering into the superconducting state.[25] Thus, excess Fe provides a local moment interacting with the Fe plane magnetism, which is expected to persist, even if the magnetism of the Fe plane is

TABLE I. Superconducting parameters of all film samples obtained through WHH analysis of the upper critical field.

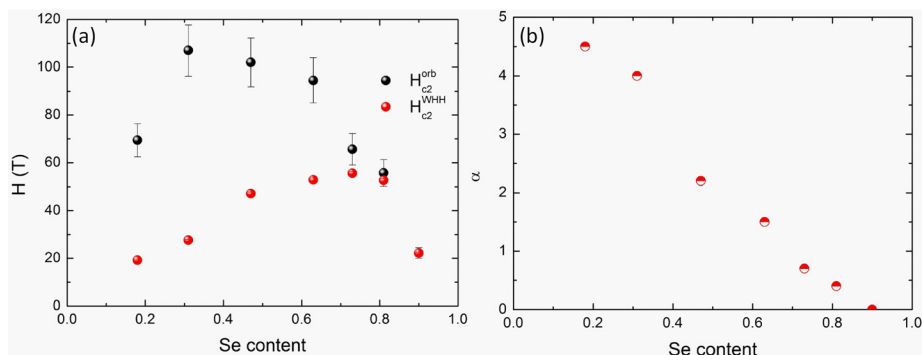| FeSe$_x$Te$_{1-x}$	$x = 0.18$	$x = 0.31$	$x = 0.47$	$x = 0.63$	$x = 0.73$	$x = 0.81$	$x = 0.90$
dH_{c2}/dt (T)	100	155	147	136	94.7	80.4	32.0
$H_{c2}^{orb}(0)$ (T)	69.4	107	102	94.5	65.6	55.7	22.2
$H_{c2}^{WHH}(0)$ (T)	19.2	27.6	47.2	52.8	55.6	52.6	22.2
T_C (K)	9.8	12.2	16.1	19.8	20.3	20.1	12.1

FIG. 4. Se composition dependence of (a) the orbit-limited upper critical field $H_{c2}^{orb}(0)$ and the fitted upper critical field $H_{c2}^{WHH}(0)$, and (b) the spin-paramagnetic effect α.

destroyed by strain or doping.[27] Such interaction could enhance the effective exchange field and spin susceptibility (χ_{sp}). Because the free energy in the normal state, F_N, decreases by the amount of $0.5\chi_{sp}\mu_0 H^2$, the enhanced χ_{sp} results in a smaller value of H_{c2}^p, at which F_N reaches the value of zero.

The orbit-limited upper critical field determined by the initial slope of H_{c2} near T_C is proportional to $(lv_F)^{-1}$, where l is the mean free path and v_F is the Fermi velocity. Thus, the large $\frac{dH_{c2}}{dt}_{t=1}$ is always attributed to the disorder effect, which gives rise to interband and/or intraband scattering and could enhance the H_{c2}^{orb} by decreasing l. Figure 5(a) displays an STM image of a FeSe$_{0.73}$Te$_{0.27}$ film with exposed Se/Te atoms arranged in a square-like lattice. The surface of this film is made up of two types of atoms, bright and dark, with a height difference of around 45 pm, as shown in Fig. 5(b). Since the anion heights of Se and Te are around 1.4 Å and 1.8 Å,[28] respectively, the height difference is attributed to the chemical contribution, i.e., different atomic sizes of Se and Te. This deduction is confirmed by the statistical analysis of the apparent height of individual atoms, as shown in the histogram of Fig. 5(d). By using the Gaussian

distribution fitting, it is found that there exists a double-peak distribution with a mean height difference of around 45 pm. The area ratio of the higher peak to the lower peak is 0.68:0.32, close to the composition ratio of Se to Te in this film. Therefore, the "dark" atom and "bright" atom are identified as Se and Te atoms, respectively. Te atoms are distributed randomly in the arrangement of Se atoms, which is expected to induce more disorder with increasing Te content due to the larger atomic size of Te compared with that of Se, resulting in a larger H_{c2}^{orb}. This inference is consistent with the transport results, where FeSe is the cleanest compound in the 11 system due to its having the largest *RRR* value and smallest residual resistivity before entering into the superconducting state. The enhancement of $\frac{dH_{c2}}{dt}_{t=1}$ or H_{c2}^{orb} would lead to the strong bending effect in $H_{c2}(t)$ curves, i.e., strong spin paramagnetic effect. It is noteworthy that there is no excess Fe in the STM results for FeSe$_{0.7}$Te$_{0.3}$, excluding the influence of Fe(2) on the spin-paramagnetic effect in high Se content samples. In fact, the amount of excess Fe is negligible when $x \geq 0.3$, in which the upturn of $R(T)$ disappears. The disorder-induced enhancement of the spin-paramagnetic effect has been observed in other IBSs. For example, the
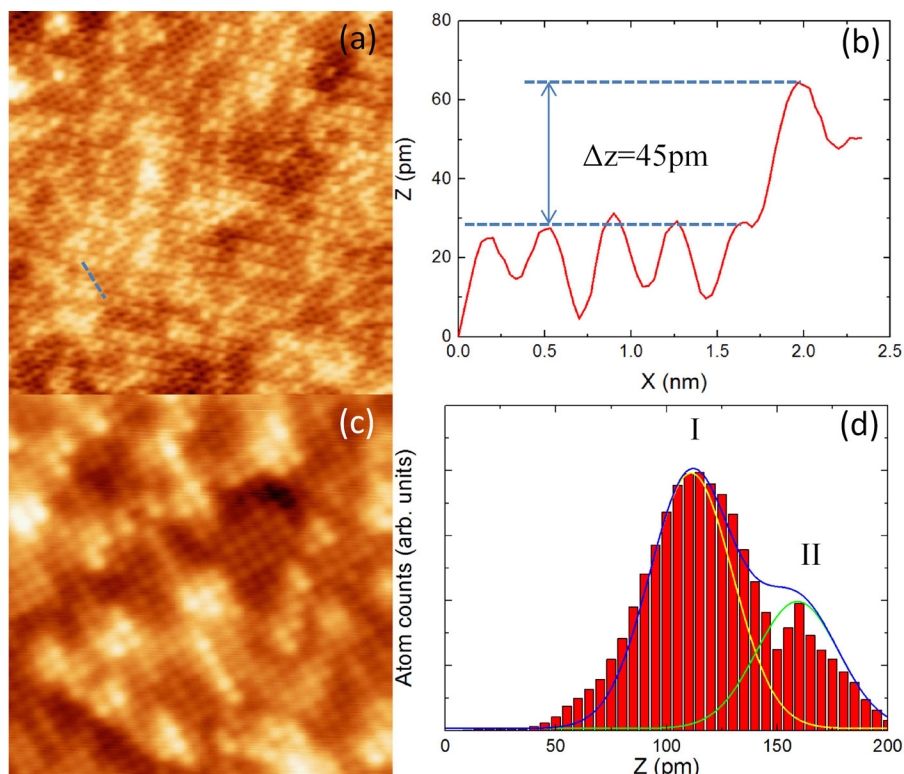

FIG. 5. (a) STM topographic image of FeSe$_{0.73}$Te$_{0.27}$ film (15 nm × 15 nm, V_{bias} = 50 mV, I_{tip} = 30 pA), (b) line profile for the blue dashed line in panel (a), (c) atomic resolution STM image (10 nm × 10 nm, V_{bias} = 300 mV, I_{tip} = 30 pA), (d) histogram of atom heights imaged in (a).

Maki parameter increased from $\alpha = 0.25$ in LaFeAsO$_{0.93}$F$_{0.07}$ to $\alpha = 1.31$ for an As-deficient La-1111 sample,[7] where the disorder induced by As deficiency provides intraband scattering, contributing to the orbit-limited upper critical field. In the case where interband scattering of Cooper pairs is enhanced by introducing disorder, the suppression of T_C is expected.[29] Nevertheless, T_C is slightly increased after Te doping in the 11 system. Consequently, the introduced disorder is assumed to scatter within the individual Fermi surface sheet, leading to the suppression of interband scattering and stabilization of the unconventional $s_\pm$ state for high T_C.[7,29]

In summary, we have investigated the doping dependence of the upper critical field in FeSe$_x$Te$_{1-x}$ thin films ($0.18 \leq x \leq 0.90$). The role of the Pauli-limited effect on $H_{c2}(t)$ is revealed in the magnetic phase diagram of FeSe$_x$Te$_{1-x}$. STM reveals that the Te doping could induce disorder, giving rise to a tunable spin-paramagnetic effect in FeSe$_x$Te$_{1-x}$. Our study sheds light on our understanding of the upper critical field, which has benefits for potential high field application of IBSs.

[1]Y. Kamihara, T. Watanabe, M. Hirano, and H. Hosono, J. Am. Chem. Soc. **130**, 3296 (2008).

[2]X. H. Chen, T. Wu, G. Wu, R. H. Liu, H. Chen, and D. F. Fang, Nature **453**, 761 (2008).

[3]Z. A. Ren, W. Lu, J. Yang, W. Yi, X. L. Shen, Z. C. Li, G. C. Che, X. L. Dong, L. L. Sun, F. Zhou, and Z. X. Zhao, Chin. Phys. Lett. **25**, 2215 (2008).

[4]J. Jaroszynski, F. Hunte, L. Balicas, Y. J. Jo, I. Raicevic, A. Gurevich, D. C. Larbalestier, F. F. Balakirev, L. Fang, P. Cheng, Y. Jia, and H. H. Wen, Phys. Rev. B **78**, 174523 (2008).

[5]H. S. Lee, M. Bartkowiak, J. H. Park, J. Y. Lee, J. Y. Kim, N. H. Sung, B. K. Cho, C. U. Jung, J. S. Kim, and H. J. Lee, Phys. Rev. B **80**, 144512 (2009).

[6]G. Fuchs, S. L. Drechsler, N. Kozlova, G. Behr, A. Köhler, J. Werner, K. Nenkov, C. Hess, R. Klingeler, J. E. Hamann-Borrero, A. Kondrat, M. Grobosch, A. Narduzzo, M. Knupfer, J. Freudenberger, B. Büchner, and L. Schultz, Phys. Rev. Lett. **101**, 237003 (2008).

[7]G. Fuchs, S. L. Drechsler, N. Kozlova, M. Bartkowiak, J. E. Hamann-Borrero, G. Behr, K. Nenkov, H. H. Klauss, H. Maeter, A. Amato, H. Luetkens, A. Kwadrin, R. Khasanov, J. Freudenberger, A. Köhler, M. Knupfer, E. Arushanov, H. Rosner, B. Büchner, and L. Schultz, New J. Phys. **11**, 075007 (2009).

[8]J. L. Zhang, L. Jiao, F. F. Balakirev, X. C. Wang, C. Q. Jin, and H. Q. Yuan, Phys. Rev. B **83**, 174506 (2011).

[9]H. Q. Yuan, J. Singleton, F. F. Balakirev, S. A. Baily, G. F. Chen, J. L. Luo, and N. L. Wang, Nature **457**, 565 (2009).

[10]S. A. Baily, Y. Kohama, H. Hiramatsu, B. Maiorov, F. F. Balakirev, M. Hirano, and H. Hosono, Phys. Rev. Lett. **102**, 117004 (2009).

[11]H. J. Kim, Y. Liu, Y. S. Oh, S. Khim, I. Kim, G. R. Stewart, and K. H. Kim, Phys. Rev. B **79**, 014514 (2009).

[12]F. C. Hsu, J. Y. Luo, K. W. Yeh, T. K. Chen, T. W. Huang, P. M. Wu, Y. C. Lee, Y. L. Huang, Y. Y. Chu, D. C. Yan, and M. K. Wu, Proc. Natl. Acad. Sci. U. S. A. **105**, 14262 (2008).

[13]M. H. Fang, H. M. Pham, B. Qian, T. J. Liu, E. K. Vehstedt, Y. Liu, L. Spinu, and Z. Q. Mao, Phys. Rev. B **78**, 224503 (2008).

[14]A. Subedi, L. Zhang, D. J. Singh, and M. H. Du, Phys. Rev. B **78**, 134514 (2008).

[15]Y. Xia, D. Qian, L. Wray, D. Hsieh, G. F. Chen, J. L. Luo, N. L. Wang, and M. Z. Hasan, Phys. Rev. Lett. **103**, 037002 (2009).

[16]S. I. Vedeneev, B. A. Piot, D. K. Maude, and A. V. Sadakov, Phys. Rev. B **87**, 134512 (2013).

[17]H. C. Lei, R. W. Hu, E. S. Choi, J. B. Warren, and C. Petrovic, Phys. Rev. B **81**, 094518 (2010).

[18]S. Khim, J. W. Kim, E. S. Choi, Y. Bang, M. Nohara, H. Takagi, and K. H. Kim, Phys. Rev. B **81**, 184511 (2010).

[19]J. C. Zhuang, W. K. Yeoh, X. Y. Cui, J. H. Kim, D. Q. Shi, Z. X. Shi, S. P. Ringer, X. L. Wang, and S. X. Dou, Appl. Phys. Lett. **104**, 262601 (2014).

[20]J. C. Zhuang, W. K. Yeoh, X. Y. Cui, X. Xu, Y. Du, Z. X. Shi, S. P. Ringer, X. L. Wang, and S. X. Dou, Sci. Rep. **4**, 7273 (2014).

[21]T. J. Liu, J. Hu, B. Qian, D. Fobes, Z. Q. Mao, W. Bao, M. Reehuis, S. A. J. Kimber, K. Prokeš, S. Matas, D. N. Argyriou, A. Hiess, A. Rotaru, H. Pham, L. Spinu, Y. Qiu, V. Thampy, A. T. Savici, J. A. Rodriguez, and C. Broholm, Nat. Mater. **9**, 718 (2010).

[22]B. Maiorov, T. Katase, S. A. Baily, H. Hiramatsu, T. G. Holesinger, H. Hosono, and L. Civale, Supercond. Sci. Technol. **24**, 055007 (2011).

[23]K. Maki, Phys. Rev. **148**, 362 (1966).

[24]N. R. Werthamer, E. Helfand, and P. C. Hohenberg, Phys. Rev. **147**, 295 (1966).

[25]T. J. Liu, X. Ke, B. Qian, J. Hu, D. Fobes, E. K. Vehstedt, H. Pham, J. H. Yang, M. H. Fang, L. Spinu, P. Schiffer, Y. Liu, and Z. Q. Mao, Phys. Rev. B **80**, 174509 (2009).

[26]W. Bao, Y. Qiu, Q. Huang, M. A. Green, P. Zajdel, M. R. Fitzsimmons, M. Zhernenkov, S. Chang, M. H. Fang, B. Qian, E. K. Vehstedt, J. H. Yang, H. M. Pham, L. Spinu, and Z. Q. Mao, Phys. Rev. Lett. **102**, 247001 (2009).

[27]L. J. Zhang, D. J. Singh, and M. H. Du, Phys. Rev. B **79**, 012506 (2009).

[28]Y. Mizuguchi, Y. Hara, K. Deguchi, S. Tsuda, T. Yamaguchi, K. Takeda, H. Kotegawa, H. Tou, and Y. Takano, Supercond. Sci. Technol. **23**, 054013 (2010).

[29]Y. Senga and H. Kontani, New J. Phys. **11**, 035005 (2009).